Polymer Degradation and Stability 105 (2014) 107–115

Contents lists available at ScienceDirect

Polymer Degradation and Stability

journal homepage: www.elsevier.com/locate/polydegstab

Determination of the thermal endurance of PCB FR4 epoxy laminates via thermal analyses

R. Polanský [a,*], P. Prosr [a], M. Čermák [b]

[a] University of West Bohemia, Faculty of Electrical Engineering, Regional Innovation Centre for Electrical Engineering, Univerzitní 8, 306 14 Pilsen, Czech Republic

[b] University of West Bohemia, Faculty of Electrical Engineering, Department of Technologies and Measurement, Univerzitní 26, 306 14 Pilsen, Czech Republic

ARTICLE INFO

Article history:
Received 27 November 2013
Received in revised form
26 March 2014
Accepted 31 March 2014
Available online 18 April 2014

Keywords:
Thermal endurance
Epoxy laminate
PCB FR4
Thermal analyses
DSC
TGA

ABSTRACT

This study evaluated new experimental parameters and end-point criteria for determining the thermal endurance of fibreglass-reinforced epoxy laminates via thermal analysis. Differential scanning calorimetry (DSC), thermogravimetric analysis (TGA), and dynamic mechanical analysis (DMA) were used in these experiments. The composite was exposed to temperatures ranging from 170 to 200 °C for times ranging from 10 to 480 h in accord with IEC 60216. The maximum heat flow temperature (DSC T_{max}) for the first thermo-oxidative reaction, the maximum weight loss temperature (DTGA T_{max}), and the maximum decomposition rate were investigated. The change in the glass transition temperature after the thermal ageing was also determined using DMA. The structural changes in the samples were examined via Fourier transform infrared spectroscopy and microscopic analysis. Oxidative degradation at the surface accompanied by pyrolytic degradation in the bulk of the sample was observed. The end-point criteria were derived for all applied methods based on the time required for the composite structure to delaminate considerably. The obtained data were used to construct Arrhenius diagrams, and cross-correlation was sought among all experimental parameters. These measurements demonstrated that the DTGA T_{max}, DMA T_g, and DSC T_{max} characterizes the ageing process sufficiently well within the applied temperature interval and satisfy the IEC 60216 requirements.

1. Introduction

Composite materials are an essential part of our world and lives. Their properties can be modified considerably, which has led to their widespread application in many industrial fields. Electrical engineering is no exception, and composite materials play an important role in this field. Composite materials must typically satisfy many requirements, i.e., excellent mechanical properties, good chemical stability, and suitable dielectric behaviour, which play an important role during their manufacture and application. Furthermore, the long-term thermo-oxidative stability directly influences the material lifetime and is used as a requirement that the composite material must fulfil. Determining the thermal endurance for the estimated service lifetime is critical during the design process of any material, whether it is the insulation system of a rotating or non-rotating machine, the dimensioning of a cable sheet, or the selection of a suitable material for printed circuit boards (PCBs).

The planned service lifetime of most engineering materials is several decades under standard operating conditions. Therefore, estimating the degradation lifetime at the operating temperature is not feasible because the necessary tests are time intensive and economically unacceptable. One possible solution is the use of accelerated ageing tests, in which the tested material is frequently exposed to an increased temperature load. Temperature itself is one of the primary degradation factors for most engineering materials, and it can accelerate the physical and chemical degradation processes within the material structure [1,2].

The normal operating temperature can be significantly exceeded in some cases, e.g., by short overloading electrical equipment or using a specific manufacturing technique. PCB laminates are one example [3,4]. Specifically, the rated load operating temperature of the PCB equipment must be distinguished from the manufacturing temperature load.

PCB laminates are commonly composed of glass fibres and an epoxy resin matrix [5–7]. During surface-mount assembly and

* Corresponding author. Tel.: +42 037 7634517; fax: +42 037 7634502.
E-mail address: rpolansk@ket.zcu.cz (R. Polanský).

http://dx.doi.org/10.1016/j.polymdegradstab.2014.03.043
0141-3910/

soldering, the PCB is exposed to temperatures significantly above the glass transition temperature (T_g) of the epoxy resin. Wave soldering overheats the PCB laminates for a short duration because the melting temperature of conventional SnPb solder is 183 °C, whereas new lead-free solders require higher temperatures of above 200 °C [3]. Considering that the glass transition temperature of a standard epoxy resin used to manufacture PCB laminates is approximately 130 °C [7] or less [8], these manufacturing techniques may shorten the service life of the composite. Lall et al. [3] has demonstrated that even short-term exposure to the high temperatures ($T > T_g$) associated with lead-free reflow processes can noticeably change the glass transition temperature of PCB laminates. He applied several soldering-temperature profiles with different variables (e.g., time above liquidus, peak temperature, ramp rate, and cooling rate) and analysed the T_g via thermo-mechanical analysis. A statistical analysis of the variables revealed the strong influence of wave soldering on T_g. Furthermore, some studies have attempted to change the structure of PCB using relatively low load temperatures with long exposure times. Lé-Magda et al. [6] have studied the influence of a temperature load of 110 °C ($T < T_g$) on a PCB throughout an exposure of 15,100 h. The structural changes were observed via differential scanning calorimetry (DSC), modulated differential scanning calorimetry (MDSC), and microscopy. Lé-Magda et al. found that thermal ageing at $T < T_g$ was caused by the thermo-oxidative reaction of material moving from the surface deeper into the material. After 500 h of accelerated ageing, a new amorphous layer was created on the composite surface that blocked further oxygen diffusion. That study proved that the ageing was governed by chemical modification over a time range of 0–7000 h, whereas ageing times longer than 7000 h have significantly decreased chemical modification rates.

The ageing mechanism at $T < T_g$ should (by its very nature) better reflect the load operating temperature because the material (except for such events as reflow processes) will be exposed to temperatures below the T_g of the epoxy resin during normal operation; however, the time consumed by these or similar experiments remains a disadvantage.

Estimating the thermal endurance of electrical insulation is no exception. Ageing experiments are time intensive and both experimentally and economically demanding. Therefore, in practice, several influences must be omitted, which can (in addition to temperature) affect the ageing process of these materials. The established methodology for determining the thermal endurance of a material used for electrical applications is found in the international standard IEC 60216 "*Guide for the determination of thermal endurance properties of electrical insulating materials*" [9], which defines all of the required test procedures. Temperature is considered to be the dominant degradation factor in this standard. For this reason, use of a higher temperature during testing (in the case of epoxy resin laminates, $T > T_g$) is recommended for comparison to normal operating conditions. Hence, the experiment duration is shortened proportionally.

The material is in a rubbery state when aged at temperatures above the T_g of the epoxy network. This state modifies the chemical bonds themselves (chemical ageing) and promotes the degradation process. In contrast, a material that is exposed to temperatures below T_g is still in a glass-like state (vitrified network) that allows for molecular movement and structural relaxation (physical ageing) [6,7]. Whenever larger sample specimens are exposed to accelerated thermal conditions, the diffusion-limited oxidation (DLO) effect must also be considered [10]. High temperatures together with the specimen geometry may result in a diffusion-limited oxygen supply in the interior of the specimens because too many chemical reactions cause a lack of oxygen within the material, leading to the evolution of spatially dependent degradation zones [11]. Accelerated thermal ageing is a question of competition between oxidative and inert degradation processes, i.e., between surface (homogeneous) and bulk (heterogeneous) degradation [11]. The intensity of thermal oxidation decreases along the specimen depth [6,12]. Moreover, diffusion is more pronounced in the rubbery state because of the higher mobility of the polymer chain segments, which allows oxygen molecules to diffuse more freely into the inner structure [12].

The ageing of epoxy resin laminates in the rubbery state ($T > T_g$) has been the subject of many studies evaluating factors other than the temperature that also affect the degradation process (e.g. [13–19]). These studies often use complex, multi-factor stress tests to separately describe the changes in all studied parameters and clarify the degradation mechanism of the epoxy resin. However, the inclusion of more stress factors can lead to non-Arrhenius behaviour of the monitored parameters [11,20–22], which prevents a simple extrapolation of the accelerated ageing data.

Nevertheless, with the rapid development of new polymer materials, these complicated modelling methods are inappropriate for rapid, routine block estimation and classification of materials into temperature classes [9,23]. However, despite the known disadvantages of this procedure [11,20], rapid thermal-endurance tests of electrical insulating materials must be performed based on measured experimental parameters according to the Arrhenius law:

$$k = A \cdot \exp\left(\frac{-E_a}{R \cdot T}\right), \tag{1}$$

where k is the reaction rate, E_a [kJ mol^{-1}] is the activation energy, R [J K^{-1} mol^{-1}] is the universal gas constant, T [K] is the absolute temperature, and A [s^{-1}] is the pre-exponential factor.

Even when simplified, the established IEC procedure has many limitations and should not be used without considering certain key issues. The international standard IEC 60216 is intended for the rapid classification of electrical insulating materials into temperature classes and does not distinguish between oxidative and inert degradation processes. The IEC procedure assumes a linear dependence between ln k and the reciprocal of the absolute temperature ($1/T$) to allow the results to be easily extrapolated to lower or higher temperatures, i.e., the procedure may fail when too large a temperature interval is examined (many materials exhibit curvature in the Arrhenius plot under these conditions [11,12]). Consequently, the standard requires not only appropriate monitored parameters but also the proper selection of the end-point criterion. The experimental parameters and end-point criteria should correspond to the ageing, and a sufficiently sensitive measurement method should be applied. When all requirements of the IEC standard are met, the resulting Arrhenius diagrams can be extrapolated to ±25 °C above or below the temperature range investigated (as for example shown later in this study). These limitations reduce most of the inaccuracies caused by mechanistic changes and DLO.

Despite the availability of this simplified testing procedure, the degradation characteristics of many commonly used materials are still unknown because of the time-consuming nature of these tests [24]. Moreover, some commonly used and recommended methods (e.g., flexural-strength testing, weight loss, breakdown voltage [9]) or proposed ageing end-point criteria are often found to be insufficient after several months of testing. Naturally, the results of these unsuccessful tests are typically not published. Hence, the examination of novel methods and the evaluation of new experimental parameters, together with the determination of end-point criteria, are necessary for the reasons given above. Cross-correlation should be established for many polymer composites and for the applied methods; however, experimentally, this is not always trivial. Obtaining this information is essential and would offer many

benefits, for example, to laboratories or manufacturers that are not equipped with all of the instruments necessary for testing the wide range of materials used in electrical engineering, among other fields. Therefore, the continuous examination of newly developed methods that are applicable to a variety of materials is crucial.

For these reasons, this study explored new potential parameters for determining the thermal endurance of a glass-reinforced flame-retardant epoxy laminate, FR4, via thermal analyses. Two different thermal analyses, differential scanning calorimetry (DSC) and thermogravimetric analysis (TGA), in addition to delamination testing, were used for these experiments. The data from the dynamic mechanical analysis (DMA, partially published previously [8]) were also used for the final evaluation of the thermal endurance. An overview of the tested laminate ageing mechanisms was also obtained using Fourier transform infrared spectroscopy and microscopy. The cross-correlation of all experimental parameters and applied methods is discussed.

2. Experimental

2.1. Descriptions of materials and thermal ageing

The examined material was a commercially available FR4 PCB laminate designed to operate at temperatures of up to 130 °C. The initial T_g of the epoxy network is 124 °C (evaluated from the peak maximum of loss modulus E'' measured via DMA). This material is a fibreglass-reinforced, flame-retardant epoxy resin laminate supplied as a sheet with a nominal thickness of 1.5 mm. The binder consists of a brominated epoxy resin that contains bisphenol A diglycidyl ether and tetrabromobisphenol A diglycidyl ether with a total bromide content of 20%. The resin was supplied in 80% methyl ketone. A combination of dicyandiamide (DCDA) with methoxypropanol and 2-methylimidazole as an accelerator was used as the hardener during manufacturing.

Specimens with a nominal size of 100 × 105 mm were prepared from laminate boards for accelerated thermal ageing and for further testing. The accelerated thermal ageing was performed in a Venticell laboratory oven (BMT Medical Technology, Brno, Czech Republic) under dry airflow.

Preliminary ageing tests, which facilitated the optimisation of the sample exposure temperatures and times, preceded the main experiment. Four test temperatures (170, 180, 190, and 200 °C) were chosen based on the recommended operating temperature of the composite and the IEC 60216 standard. The pre-samples were aged at the defined temperatures, and their conditions were continuously monitored. Once delamination was observed at a macroscopic level, the preliminary tests were terminated, and the delamination times for each temperature were recorded. Thus, the exposure times (Table 1) for the main experiment were estimated.

2.2. Method description

The measurements were performed via DSC and TGA on a TA Instruments SDT Q600 thermal analyser. Each compact sample was scratched in the crosswise direction of the test specimens and sieved to a 100 mesh grain size (nominal sieve opening of 0.149 mm). The primary reason for this preparation of the samples was to minimise the DLO effect. The sample weight was 12 ± 0.01 mg. During testing, the samples were placed in an open platinum pan and linearly heated at a rate of 10 °C/min from 30 °C to 700 °C in dry air with a flow rate of 100 ml/min. Three samples were analysed for each thermal ageing level (i.e., measurement frequency $n = 3$). Powdered samples were also measured via the attenuated total reflectance (ATR) FT-IR technique using the middle-infrared (IR) region to determine any changes in the epoxy matrix structure. These infrared spectra were recorded using a Nicolet 380 spectrometer with a Smart MIRacle single-reflection ATR cell (diamond crystal) with 32 average scans of 4 cm^{-1} in resolution collected across a frequency range of 4000–600 cm^{-1} for each measured spectrum. The powder was measured at a measurement frequency of 10 ($n = 10$; each spectrum was measured using a different powder). The measured data were subsequently analysed using the OMNIC spectroscopy software. The microscopic analysis was performed using an Olympus MX51 optical microscope in the fluorescence mode. Scratch patterns were prepared from the samples (vertical to the sample surface), and their structure was subsequently analysed.

Table 1
Delamination times and summary of the temperatures and times used for the thermal treatment.

Ageing temperature [°C]	Delamination time [h]	Ageing times [h]
170 °C	624	96, 192, 288, 384, 480
180 °C	180	48, 96, 120, 144, 168
190 °C	90	24, 48, 60, 72, 84
200 °C	33	10, 15, 20, 25, 30

2.3. Evaluation of the results

Fig. 1 provides an example DSC and TGA measurement (sample exposed to 170 °C for 96 h). This analysis revealed the thermal decomposition of the epoxide binder (mass residue of approximately 53% at 700 °C, which corresponded to the unfired glass-fibre content). The binder decomposition proceeded in two stages, as expected [25,26]. These results indicate two strong exothermic phenomena in the DSC curve with a local maximum ranging from 327 °C to 480 °C. These reactions were accompanied by two major reductions in the sample weight. The cause of the first decomposition reaction was the decomposition of large polymer chain segments either already created in the matrix or formed at the onset of the thermal destruction of the structure. The second exotherm was associated with the decomposition of the carbonised products [26].

The data analysis focused on the first decomposition reaction and the determination of which new parameters would be suitable for evaluating the thermal endurance of the material from the thermal analyses. The second decomposition reaction (total destruction of all carbonised products) is not suitable for this purpose because of its variability. To emphasise each effect, the derivative of the

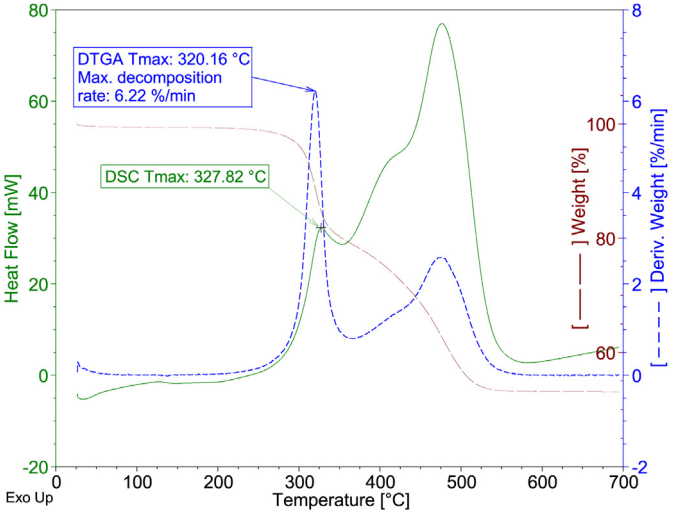

Fig. 1. DSC, TGA, and DTGA traces for a sample aged for over 96 h at 170 °C.

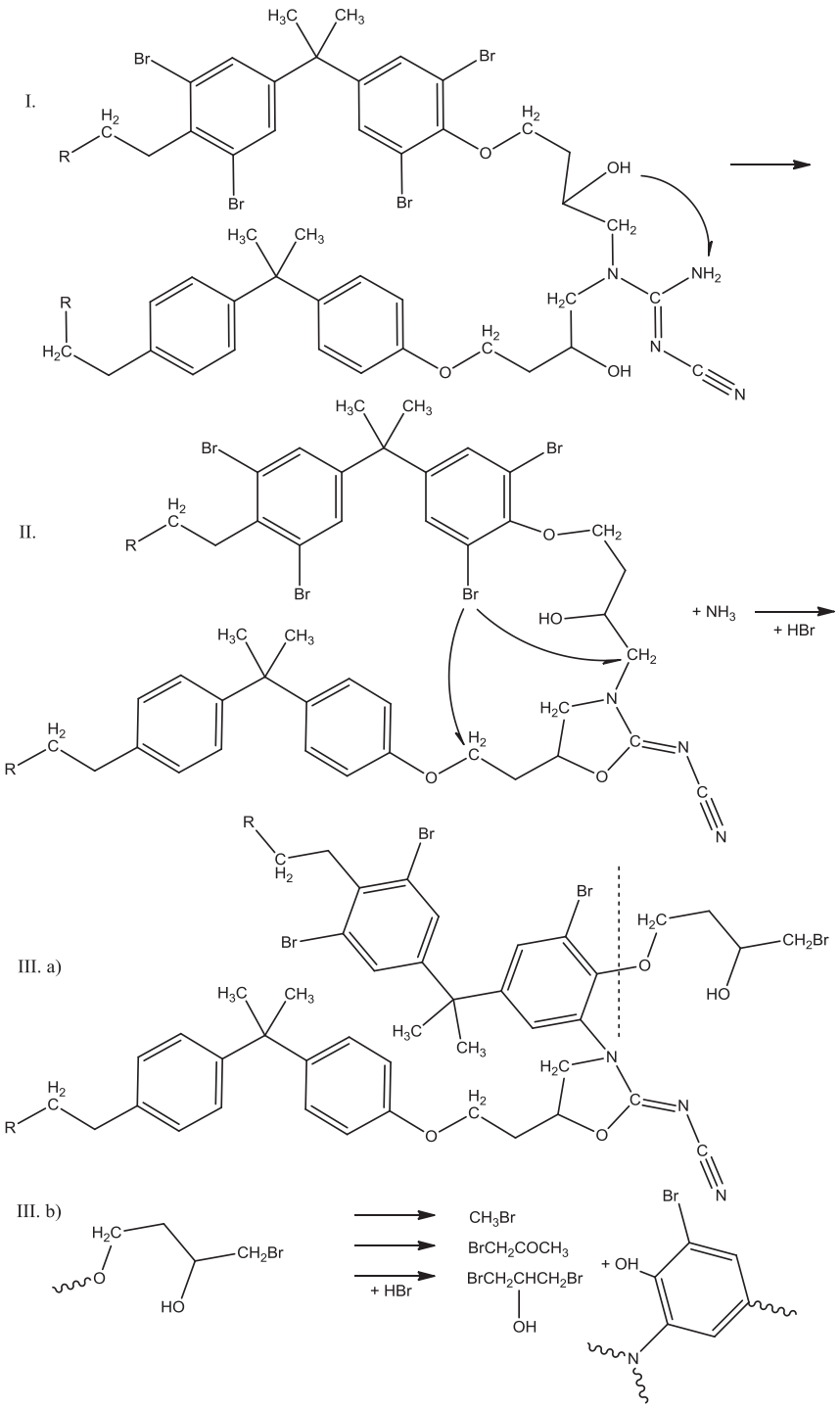

Fig. 2. Chemical processes assumed to contribute to thermal degradation in the ideal situation for brominated epoxy resin cured with DCDA.

thermogravimetric analysis data was plotted (DTGA). The first local maximum in this curve, DTGA T_{max} (i.e., the maximum weight loss temperature), occurred at a slightly lower temperature than the first peak maximum in the DSC curve, labelled DSC T_{max} (i.e., the maximum heat flow temperature for the first reaction). The maximum decomposition rate (in %/min) of the binder during this reaction was reached before the main heat release. The mutual relation of the TGA and DSC results is expected because weight loss is accompanied by heat release during oxidative epoxy degradation. However, each method probes a different aspect of the degradation, and the two methods may provide results of different sensitivities. Hence, the DTGA T_{max}, DSC T_{max}, and maximum decomposition rate were all considered for further evaluation because they precisely characterise the first decomposition reaction.

3. Results and discussion

3.1. Thermo-oxidative ageing of brominated epoxy resin: assumptions

The thermo-oxidative ageing process for brominated epoxy resins is thoroughly described in Refs. [25–30]. The laminates are

thermally cured via the reaction of epoxy resins with dicyandiamide at 180 °C. At sufficient pressure, the curing process begins to cycle, and the structural arrangement changes frequently via the exclusion of ammonia (Fig. 2, Scheme I) [27].

During long-term thermal ageing, the dehydration of secondary alcohols occurs [25] before the destruction of the structure in areas with weak alkyl bonds (Fig. 2, Schemes II and III.a) [28]. In this situation, these bonds are more susceptible to nucleophilic substitution and can easily form HBr. Moreover, HBr can destabilise its surroundings. This destabilisation contributes significantly to the initialisation of other important chemical reactions, such as intramolecular abstractions or the formation of aromatic alkyl substituents, which creates the remaining amino groups on the cleaved molecules [29]. However, the formation of methyl bromide, 1,3-bromoacetone, dibromopropane, and phenolic groups (Fig. 2, Scheme III.b) dominates the initial structural decomposition. These radicals subsequently disrupt the material integrity in areas with weaker ternary boundaries, particularly in non-brominated areas. The major structural decomposition processes occur via these mechanisms [28]. Kagathara and Parsania [30] have demonstrated that these processes occur en masse at temperatures exceeding 275 °C (first thermo-oxidative reactions in the DSC curve) and cause a significant weight reduction in the material under heat stress. In particular, aliphatic hydrocarbon residues and ketones form during these reactions. However, the boiling temperatures of most by-products produced during thermal ageing are below 150 °C. Therefore, the high level of mobility and also the reactivity of the by-products should be reflected at all temperatures during the experiment. This theoretical basis leads to the hypothesis that prolonged thermal stress significantly affects the material integrity, thereby weakening the first exothermic reaction. The glass transition temperature may decrease because of the structural fragmentation of the material because the structure will not be as chemically self-linked as it was prior to the heat stress.

3.2. Influence of thermal ageing on the material structure

The effect of thermal stress testing on the material structure was first documented via FT-IR. The FT-IR spectra of the as-delivered material and a representative set of samples aged at 170 °C are presented in Fig. 3. The sample ageing process is correlated with the spectral band at 1737 cm^{-1}, which corresponds to the stretching vibration of the C=O carbonyl group. An increase in the intensity of this band indicates the partial oxidation of the tested material as a result of the ageing process. Another confirmation of the ageing process was observed as the changes in intensity of the bands at 1606 cm^{-1} (ν_{asym} aromatic CCH) and 1507 cm^{-1} (from the conjugation of the benzene substituent) [7,31]. These changes correspond to Scheme III.b in Fig. 2.

Microscopic analysis can assist in exploring ageing mechanisms in a visual manner. Microscopic images of the same data set (the set of samples aged at 170 °C) are shown in Fig. 4. Although thermo-set materials such as highly cross-linked epoxies seem to tolerate significant oxidation levels [11], it is clear that the structure of PCB laminates is affected in such highly oxidative pyrolytic conditions. The ageing of PCB FR4 in air initiates the expressive oxidation process [6,32], which proceeds throughout the sample over time. The results of microscopic analysis indicate the gradual thermo-oxidative heterogeneous degradation of the epoxy resin on the sample surface. As evidence of this process, although the laminate structure became oxygen-diffusion limited at the surface–air interface, the thermal ageing caused the gradual formation of an increasingly thicker diffusion layer for thermal oxidative degradation. The colour intensity inside the specimen also gradually changed in a manner that was clearly related to the bulk (homogeneous) degradation process, which caused inert pyrolytic decomposition in the laminate interior.

The results of the microscopy illuminate the role played by fibreglass in the degradation process. It is evident (primarily for specimens aged for 384 and 480 h; see Fig. 4) that the fibreglass reinforcement contributed to the retardation of the rate of diffusion of thermo-oxidative degradation towards the interior. The typical

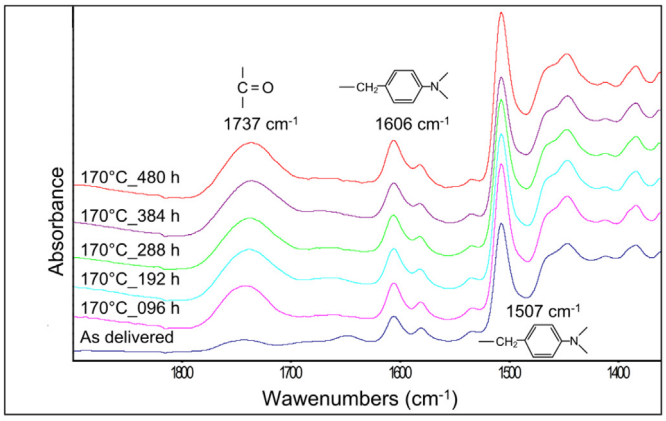

Fig. 3. FT-IR spectra of specimens treated at 170 °C.

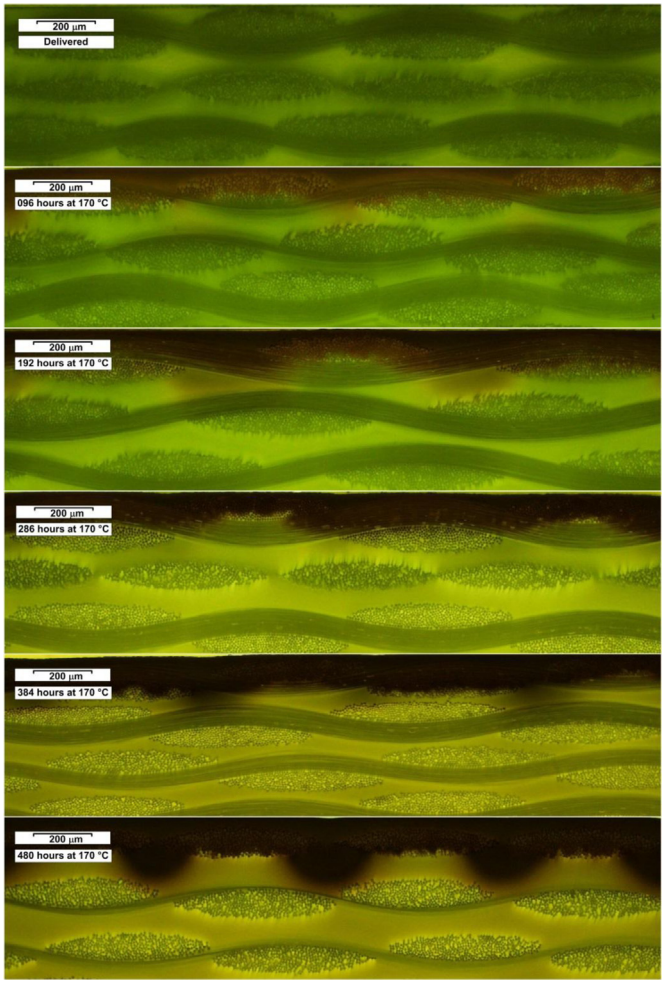

Fig. 4. Discolouration of the specimens treated at 170 °C (scratch patterns).

thermal conductivity of common PCB FR4 epoxy resin systems is approximately 0.2–0.34 W/(m K) [33,34], whereas the thermal conductivity of the fibreglass is an order of magnitude lower than that of PCB FR4 epoxy systems (0.02–0.04 W/(m K)) [35]. This significant difference in thermal conductivity between the epoxy resin system and the fibreglass can limit the heat transfer and, more importantly, slow the release of decomposition by-products from the structure, and vice versa. Hence, the fibreglass can play an important role in the competition between oxidative and inert degradation processes. Nevertheless, when the thermal ageing reached a certain level, the oxidation process passed through the fibreglass mesh, and the material began to delaminate at the fibre–resin interface (regions of orthogonally overlapping fibres are the most strongly affected). During operation, the degraded regions led to the gradual deterioration of both the mechanical and electrical properties of the material and subsequently destroyed the laminate.

3.3. TGA And DSC results

Only the set of samples aged at 170 °C is represented in the following figures. The TGA results are shown in Fig. 5. The slope reduction and gradual decline of the TGA curves indicate a change in the proportion of the crystalline phase in the structure and fragmentation of the epoxy system according to the duration of the applied thermal ageing. Both stages of decomposition were affected; the first decomposition reaction was affected by the early stages of ageing (up to 384 h), whereas the second decomposition reaction was sensitive to longer ageing times (288–480 h).

As shown in Fig. 6, the point in the weight-loss curve with the greatest rate of change (maximum decomposition rate) primarily reflects the kinetics of the first decomposition reaction, which dominates the initial structural decomposition (formation of methyl bromide, 1,3-bromoacetone, dibromopropane, and phenolic groups; see Fig. 2, Scheme III.b). As the structure of the epoxy network fragmented because of the thermal ageing, the maximum decomposition rate decreased distinctly. The accelerated ageing also caused a slight decrease in the maximum weight loss temperature (DTGA T_{max}), which reflected a decrease in the thermal stability associated with the cross-linking density of the epoxy network. In contrast, the rate of the second decomposition reaction

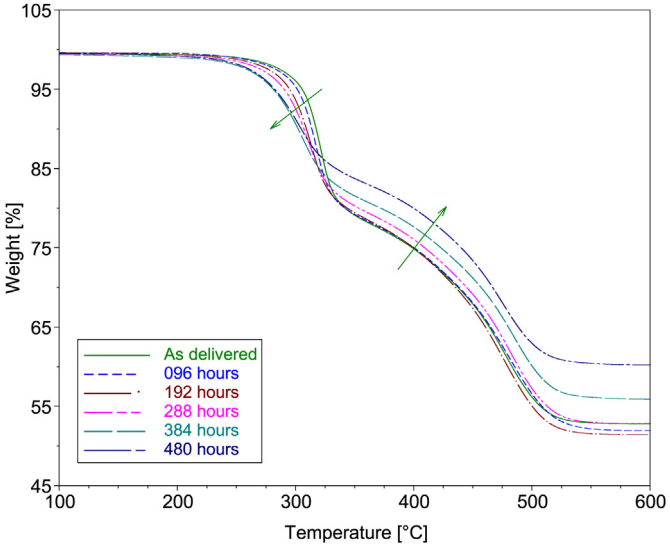

Fig. 5. TGA curves for samples treated at 170 °C.

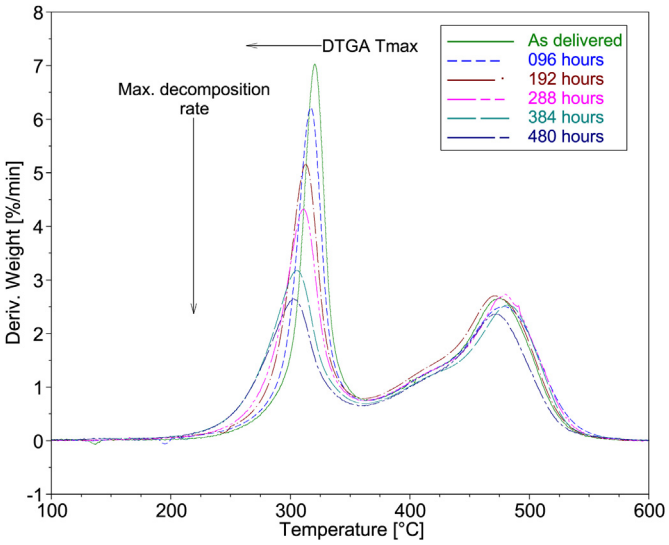

Fig. 6. DTGA curves for samples subjected to thermal treatment at 170 °C.

(at 370–550 °C) was not affected by accelerated ageing. Of course, it is possible that the structure of the material is completely destroyed at such high temperatures.

The DSC results (shown in Fig. 7) correlate well with those of TGA and DTGA, as expected. The accelerated ageing influenced only the first decomposition reaction, gradually decreasing the heat released and lowering the highest DSC T_{max} peak with increased ageing.

3.4. Discussion of trends

At first glance, all parameters described in the previous paragraph clearly reflect the ageing process, but there are some considerations that must be taken into account when a new experimental parameter is evaluated. First of all, experimental parameters that change linearly with ageing are preferred. Such parameters can be easily linearly fitted, allowing the time to the end-point criterion to be calculated precisely. Parameters that exhibit non-linear behaviour can also be used, but in such cases, more sophisticated curve fitting is required, which sometimes results in lower accuracy. Moreover, the statistical significance of the curve fitting should be considered. One of the many methods of doing so is to test the significance of the coefficient of correlation, R (or coefficient of determination, R^2) [36–38], when the value of the two-tailed test criterion, t, for a specific number of degrees of freedom is calculated using the following equation:

$$t = \frac{R \cdot \sqrt{n-2}}{\sqrt{1-R^2}}, \qquad (2)$$

where n is the sample size (number of measured points used for curve fitting), R is the coefficient of correlation, and R^2 is the coefficient of determination.

The calculated test criterion, t, must then be greater than the critical value of the test criterion [39,40], $t_{crit.}$ (probability point of the complement of the cumulative distribution function of Student's t-distribution), which can be easily found in any table of Student's t-distribution (e.g., [40]).

The results presented in Figs. 5–7 and those obtained for the remaining ageing temperatures were subjected to further analysis. The changes in the monitored parameters for each temperature and ageing time are shown in Figs. 8–10. The glass transition

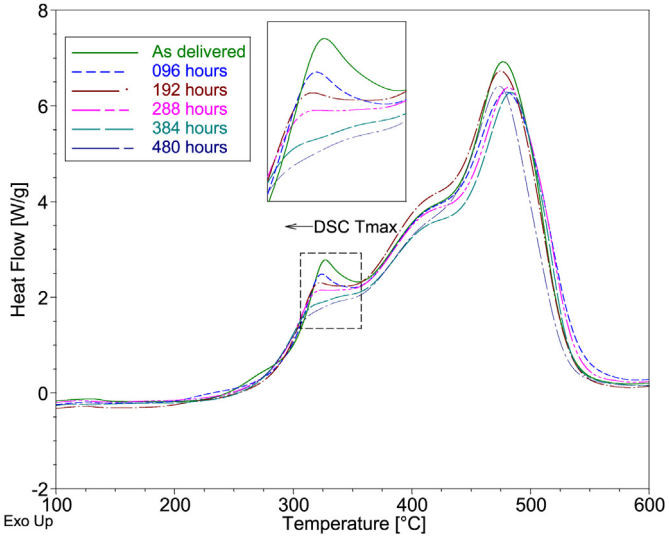

Fig. 7. DSC curves for samples subjected to thermal treatment at 170 °C.

temperature measurements (Fig. 11) obtained in a previous dynamic mechanical analysis [8] were used for the subsequent construction of linearised Arrhenius diagrams. The error bars correspond to the calculated standard deviations of the measured parameters (measurement frequency of $n = 3$), and the coefficients of determination, R^2, of the linear trend lines are also plotted in all graphs.

The variances in the DTGA T_{max} (Fig. 8) and DSC T_{max} (Fig. 10) at 170 °C were higher but remained acceptable for the relatively low measurement frequency. Generally, most of the R^2 values are greater than 0.90, indicating satisfactory relations between the evaluated parameters and the selected linear regressions. Testing for the significance of the coefficient of determination, R^2, was performed using Eq. (2). The results are summarised in Table 2. The value of $t_{crit.} = 3.182$, corresponding to three degrees of freedom (see Ref. [40]), was lower than the calculated test criteria for all considered parameters. Hence, statistically significant relations exist between the evaluated parameters and the selected linear regressions. Indeed, the trend in the maximum decomposition rate (Fig. 9 and corresponding t values in Table 2) is surprising because the results did not yield the expected linearity, despite the initially promising trends (shown in Fig. 6). The kinetics of the first decomposition reaction changed slightly at an ageing temperature

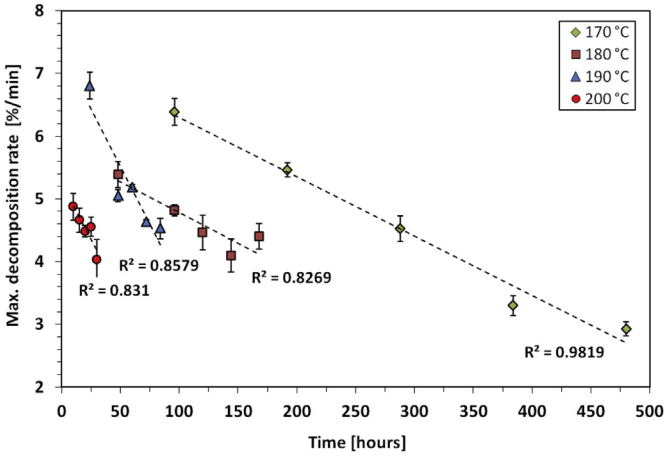

Fig. 9. DTGA – evaluation of the maximal decomposition rate.

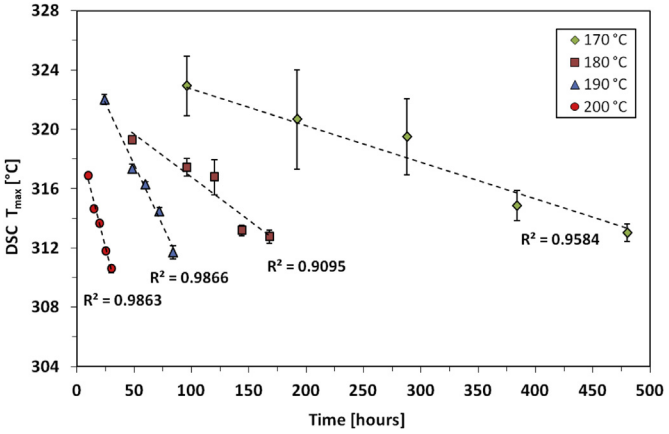

Fig. 10. DSC – evaluation of the DSC T_{max}.

of 180 °C, and the differing slope of the maximum decomposition rate and the relatively low t values reflect this behaviour. Consequently, the maximum decomposition rate was not considered for the subsequent construction of Arrhenius diagrams. In contrast, the standard deviations of the T_g values measured via DMA (Fig. 11) are the lowest of all applied methods, and the calculated t values are the most consistent. A decrease in the epoxy network T_g indicates

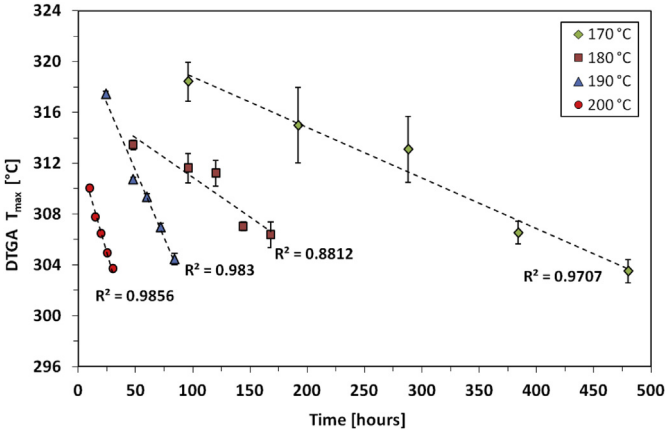

Fig. 8. DTGA – evaluation of the DTGA T_{max}.

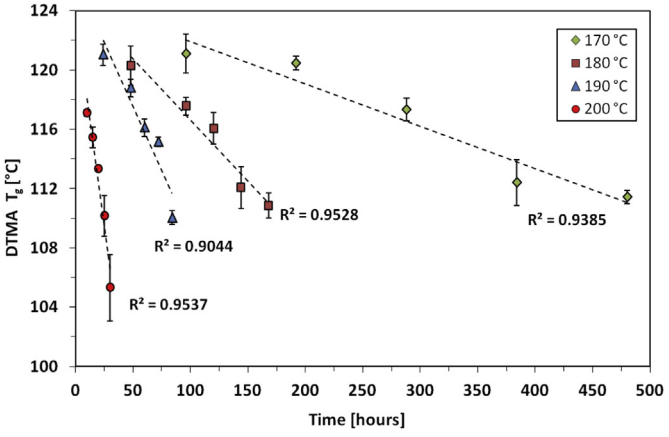

Fig. 11. DMA – evaluation of T_g (published in Ref. [8]).

Table 2
Calculated values of the two-tailed testing criterion for all experimental parameters ($t_{crit.} = 3.182$).

Ageing temperature [°C]	DTGA T_{max}		Max. decomp. rate		DSC T_{max}		DMA T_g	
	R^2	t	R^2	t	R^2	t	R^2	t
170	0.97	10.75	0.98	12.76	0.96	8.31	0.94	6.77
180	0.88	4.72	0.80	3.49	0.91	5.49	0.95	7.78
190	0.98	13.17	0.85	4.11	0.99	14.86	0.90	5.33
200	0.99	14.33	0.91	5.51	0.99	14.70	0.95	7.86

the ongoing degradation of the polymer network in the binder, which becomes susceptible to thermal stress.

3.5. Arrhenius diagrams

Arrhenius diagrams (Fig. 12) were constructed for each of the evaluated parameters. Such diagrams require knowledge of the end-point criteria. The times required for the macroscopic decomposition of the test material were used for this purpose (see Table 1). The time required to delaminate at 200 °C (i.e., 33 h) was used for the indirect deduction of the end-point criterion for each parameter. The ageing criteria for the other methods were then calculated via linear fitting based on the delamination time. The DSC T_{max} (310 °C), DTGA T_{max} (302 °C), and DMA T_g (110 °C) were then used as the end-point criteria.

The activation energies (E_a) of the degradation processes were calculated from the Arrhenius diagrams based on the slopes of the primary (measured) data. The absolute values of E_a do not greatly differ, considering the fact that the data were obtained in different manners. The Arrhenius diagrams within the applied temperature interval (170–200 °C) seem to lack any express curvature. These observations suggest that the mechanism of degradation remained unchanged throughout the evaluated temperature range. All curves were linearly fitted and then extrapolated to lower and higher temperatures, ±25 °C (the maximum possible extrapolations according to the IEC standard).

The testing for the significance of the coefficient of determination, R^2, was performed prior to extrapolation. The calculated values of the two-tailed test criterion, t, are summarised in Table 3, where the critical value of the test criterion, $t_{crit.}$, is provided in the legend. The condition $t > t_{crit.}$ is valid for all experimental parameters. Although all parameters correlate well with each other within the primary data, the extrapolation produced a slightly

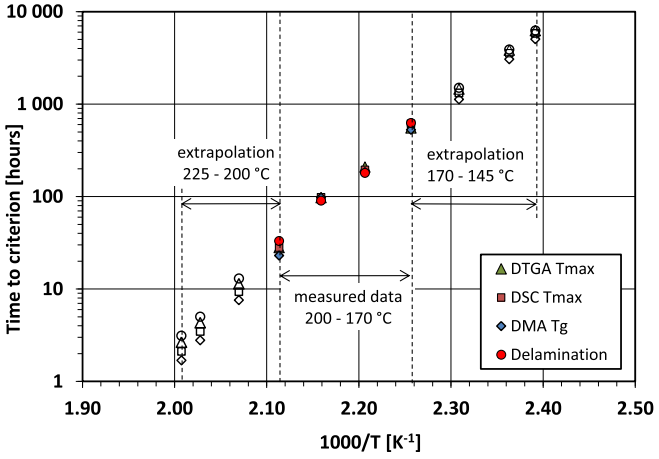

Fig. 12. Arrhenius plots for all evaluated parameters.

Table 3
Calculated values of E_a, t, and R^2 for Arrhenius diagrams (all values based on primary data; $t_{crit.} = 4.303$).

	DTGA T_{max}	DSC T_{max}	DMA T_g	Delamination
E_a [kJ/mol]	169	173	175	166
R^2	0.993	0.989	0.981	0.986
t	16.84	13.41	10.16	11.87

greater divergence. At higher temperatures, the different merits of the various parameters become particularly evident. Nevertheless, partial data divergence is to be expected because TGA and DSC probe primarily the surface oxidation of particle fragments, whereas DMA measures the T_g of a bulk sample aged in air as an average over the cross section of the sample, and delamination is a bulk property that is driven primarily by purely inert pyrolytic decomposition in the interior. Despite these differences, all these parameters can serve as proxies for the delamination or other testing within the limited temperature regime considered here and may be useful for the rapid determination of the thermal endurance of PCB FR4 epoxy laminates.

4. Conclusion

The thermal endurance of PCB FR4 epoxy laminate was studied via thermal analyses. The applied thermal ageing significantly affected the structure of the FR4 laminates, as evaluated via FT-IR, microscopy, and thermal analyses. The obtained results demonstrated that the laminate structure became oxygen-diffusion limited at the surface–air interface. The thermal ageing caused the gradual formation of an increasingly thicker diffusion layer for thermal oxidative degradation. The interior of the specimens was also gradually changed by ageing. The changes inside the laminate were clearly related to bulk (homogeneous) degradation processes, which cause inert pyrolytic decomposition. The microscopy results assisted in elucidating the role played by fibreglass in the degradation process and suggested that the difference in thermal conductivity between the epoxy resin system and the glass fibres limits the heat transfer and, more importantly, retards the release of decomposition by-products from the structure, and vice versa.

The results of TGA and DSC indicated two stages of decomposition. The slope reduction and gradual decline of the TGA curves indicated a change in the proportion of the crystalline phase in the structure and the fragmentation of the epoxy system according to the duration of the applied thermal ageing. As the structure of the epoxy network fragmented because of the thermal ageing, the maximum decomposition rate distinctly decreased. The accelerated ageing also caused a slight decrease in the maximum weight loss temperature, which reflected a decrease in the thermal stability associated with the cross-linking density of the epoxy network. The DSC results are well correlated with those of TGA, as expected. The accelerated ageing influenced only the first decomposition reaction, gradually decreasing the heat released and lowering the highest DSC T_{max} peak with increased ageing. The glass transition temperature measured via DMA also decreased because of the structural fragmentation of the material. All experimental parameters were newly evaluated for determining the thermal endurance of fibreglass-reinforced epoxy laminates in accord with the IEC standard.

The constructed Arrhenius diagrams and calculated activation energies for the degradation process confirmed that comparable results can be achieved using all of the applied thermal analyses. During the experiments, the end-point criteria for each of the above parameters were deduced from the observed times required for macroscopic delamination.

The reported results are important to the determination of the thermal endurance for materials with a composition similar to that of the tested material. The constructed Arrhenius diagrams can assist in estimating the thermal endurance at elevated temperature whenever necessary, e.g., for evaluation of the impact of wave soldering or short overloading of electrical equipment. The proposed experimental parameters, as determined via thermal analyses, provide promising alternatives to other commonly used and recommended parameters (e.g., bending strength, breakdown voltage, and time to delamination [9]).

Acknowledgements

This research was supported by the European Regional Development Fund and the Ministry of Education, Youth, and Sports of the Czech Republic under the Regional Innovation Centre for Electrical Engineering (RICE), Project No. CZ.1.05/2.1.00/03.0094. The authors also thank Ing. Tomáš Džugan for providing pictures of the inner structures of the test materials.

References

[1] Montanari G. Notes on theoretical and practical aspects of polymeric insulation aging. IEEE Electr Insul M 2013;29(4):34–44. http://dx.doi.org/10.1109/MEI.2013.6545258.
[2] Boucher V, Rain P, Teissedre G, Schlupp P. Annu Rep Conf Electr Insulation Dielectr Phenom 2008;2008:83–6. http://dx.doi.org/10.1109/CEIDP.2008.4772842.
[3] Lall PV, Narayan J, Suhling J, Blanche J, Strickland M. 13th Intersoc Conf Therm Thermomech Phenom Electron Syst 2012;2012:261–8. http://dx.doi.org/10.1109/ITHERM.2012.6231439.
[4] Lin Y, Jin C, Fang HXN. Effects of ultrasonic bonding process on polymer-based anisotropic conductive film joints in chip-on-glass assemblies. Polym Test 2011;30(3):318–23. http://dx.doi.org/10.1016/j.polymertesting.2010.12.006.
[5] Li J, Duan H, Yu K, Wang S, Strickland M. Interfacial and mechanical property analysis of Waste printed circuit boards subject to thermal shock. J Air Waste Manag Assoc 2010;60(2):229–36. http://dx.doi.org/10.3155/1047-3289.60.2.229.
[6] Lé-Magda M, Dargent E, Puente JAS, Guillet A, Font E, Saiter JM. Influence of very long aging on the relaxation behavior of flame-retardant printed circuit board epoxy composites under mechatronic conditions. J Appl Polym Sci 2013;120(2):786–92. http://dx.doi.org/10.1002/APP.39216.
[7] Lé-Magda M, Dargent E, Youssef B, Guillet A, Idrac J, Saiter JM. Macromol Symp 2012;315(1):143–51. http://dx.doi.org/10.1002/masy.201250518.
[8] Polanský R, Mentlík V, Prosr P, Sušír J. Influence of thermal treatment on the glass transition temperature of thermosetting epoxy laminate. Polym Test 2009;28(4):28–436. http://dx.doi.org/10.1016/j.polymertesting.2009.03.004.
[9] IEC 60216 guide for the determination of thermal endurance properties of electrical insulating materials. Parts 1–7. Geneva: IEC; 2002, ISBN 0-580-39048-9.
[10] Celina MC, Quintana A. A perspective on the inherent oxidation sensitivity of epoxy materials. Polymer 2013;54(13):3290–6. http://dx.doi.org/10.1016/j.polymer.2013.04.042.
[11] Celina MC. Review of polymer oxidation and its relationship with materials performance and lifetime prediction. Polym Degrad Stab 2013;98(12):2419–29. http://dx.doi.org/10.1016/j.polymdegradstab.2013.06.024.
[12] Anderson BJ. Thermal stability and lifetime estimates of a high temperature epoxy by T_g reduction. Polym Degrad Stab 2013;98(11):2419–29. http://dx.doi.org/10.1016/j.polymdegradstab.2013.08.001.
[13] Mercier J, Bunsell A, Castaing P, Renard J. Characterisation and modelling of aging of composites. Compos Part A 2008;39(2):428–38. http://dx.doi.org/10.1016/j.compositesa.2007.08.015.
[14] Ghasemzadeh S, Haddadi-Asl V, Kajorncheappunngam S, Gangarao HVS, Gupta RK. Dynamic mechanical study of epoxy, epoxy/glass, and glass/epoxy/wood hybrid composites aged in various media. Polym Compos 2009;30(12):1761–70. http://dx.doi.org/10.1002/pc.20741.
[15] Plonka R, Mäder E, Gao SL, Bellmann C, Dutschk V, Zhandarov S. Adhesion of epoxy/glass fibre composites influenced by aging effects on sizings. Compos Part A 2004;35(10):1207–16. http://dx.doi.org/10.1016/j.compositesa.2004.03.005.
[16] Ciutacu S, Budrugeac P, Niculae I. Accelerated thermal aging of glass-reinforced epoxy resin under oxygen pressure. Polym Degrad Stab 1991;31(3):365–72. http://dx.doi.org/10.1016/0141-3910(91)90044-R.
[17] Dubois C, Monney L, Bonnet N, Chambaudet A. Degradation of an epoxy-glass-fibre laminate under photo-oxidation/leaching complementary constraints. Compos Part A 1999;30(3):361–8. http://dx.doi.org/10.1016/S1359-835X(98)00104-3.
[18] Tsotsis TK, Lee SM. Long-term thermo-oxidative aging in composite materials: failure mechanisms. Compos Sci Technol 1998;58(3–4):355–68. http://dx.doi.org/10.1016/S0266-3538(97)00123-1.
[19] Barjasteh E, Bosze EJ, Tsai YI, Nutt SR. Thermal aging of fiberglass/carbon-fiber hybrid composites. Compos Part A 2009;40(12):2038–45. http://dx.doi.org/10.1016/j.compositesa.2009.09.015.
[20] Celina M, Gillen KT, Assink RA. Accelerated aging and lifetime prediction: review of non-Arrhenius behaviour due to two competing processes. Polym Degrad Stab 2005;90(3):395–404. http://dx.doi.org/10.1016/j.polymdegradstab.2005.05.004.
[21] Gillen KT, Bernstein R, Derzon DK. Evidence of non-Arrhenius behaviour from laboratory aging and 24-year field aging of polychloroprene rubber materials. Polym Degrad Stab 2005;87(1):57–67. http://dx.doi.org/10.1016/j.polymdegradstab.2004.06.010.
[22] Gugumus F. Effect of temperature on the lifetime of stabilized and unstabilized PP films. Polym Degrad Stab 1999;63(1):41–52. http://dx.doi.org/10.1016/S0141-3910(98)00059-7.
[23] Ohta S. Temperature classes of electrical Insulators [online]. Three Bond Tech News. Available from: http://www.threebond.co.uk/Portals/0/tech13.pdf; 1985 [2014-03-14].
[24] Gillen KT, Celina M, Clough RL, Wise J. Extrapolation of accelerated aging data Arrhenius or erroneous? Trends Polym Sci 1997;5(8):250–7.
[25] Luda M, Balabanovich P, Zanetti AI, Guarantto MD. Thermal decomposition of fire retardant brominated epoxy resins cured with different nitrogen containing hardeners. Polym Degrad Stab 2007;92(6):1088–100. http://dx.doi.org/10.1016/j.polymdegradstab.2007.02.004.
[26] Cascaval CN. Thermal degradation of *p*-nonylphenol formaldehyde epoxy resins. Eur Polym J 1994;30(8):969–73. http://dx.doi.org/10.1016/0014-3057(94)90033-7.
[27] Gilbert MD, Schneider NS, MacKnight WJ. Mechanism of the dicyandiamide/epoxide reaction. Macromolecules 1991;24(2):360–9. http://dx.doi.org/10.1021/ma00002a004.
[28] Balabanovich AI, Hornung A, Merz D, Seifert H. The effect of a curing agent on the thermal degradation of fire retardant brominated epoxy resins. Polym Degrad Stab 2004;85(1):713–23. http://dx.doi.org/10.1016/j.polymdegradstab.2004.02.012.
[29] Smith M, March J. In: March's advanced organic chemistry: reactions, mechanisms, and structure. 6th ed. New Jersey: John Wiley & Sons, Inc.; 2007.
[30] Kagathara VM, Parsania PH. Thermal analysis of cured halogenated epoxy resins based on bisphenol-C. Polym Test 2002;21(2):181–6. http://dx.doi.org/10.1016/S0142-9418(01)00067-8.
[31] Edwards HGM, Falk MJP. Fourier-transform Raman spectroscopic study of unsaturated and saturated waxes. Spectrochim Acta, Part A 1997;53(14):2685–94. http://dx.doi.org/10.1016/S1386-1425(97)00161-3.
[32] Damian C, Espuche E, Escoubes M. Influence of three ageing types (thermal oxidation, radiochemical and hydrolytic ageing) on the structure and gas transport properties of epoxy–amine networks. Polym Degrad Stab 2001;72(3):447–58. http://dx.doi.org/10.1016/S0141-3910(01)00045-3.
[33] Azar K, Graebner JE, Witting PA. Twelfth Ann IEEE Semiconductor Therm Measure Manage Symp Proc 1996;19(12):169–82. http://dx.doi.org/10.1109/STHERM.1996.545107.
[34] Sarvar F, Poole NJ, Witting PA. PCB glass-fibre laminates: thermal conductivity measurements and their effect on simulation. J Electron Mater 1990;19(12):1345–50. http://dx.doi.org/10.1007/BF02662823.
[35] Kostikov VI. Soviet advanced composites technology series, composite materials components. London: Chapman; 1994. p. 694.
[36] Snedecor GW, Cochran WG. In: Statistical methods. 8th ed. Ames: Iowa State University Press; 1989.
[37] Panofsky HA, Brier GW. Some applications of statistics to meteorology. Pennsylvania: Pennsylvania State University; 1958.
[38] Pearson ES. The test of significance for the correlation coefficient. J Am Stat Assoc 1931;26(174):128–34. http://dx.doi.org/10.1080/01621459.1931.10503208.
[39] Forbes C, Evans M, Hastings N, Peacock B. In: Statistical distributions. 4th ed. New Jersey: Wiley; 2011.
[40] Table of Student's *t*-distribution [online]. San José State University; 2007. Available from: http://www.sjsu.edu/faculty/gerstman/StatPrimer/t-table.pdf [2014-03-14].